



Exploring Curved Anatomic Structures with Surface Sections

Laurent Saroul Sebastian Gerlach Roger D. Hersch

Ecole Polytechnique Fédérale de Lausanne*, Switzerland

Abstract

The extraction of planar sections from volume images is the most commonly used technique for inspecting and visualizing anatomic structures. We propose to generalize the concept of planar section to the extraction of curved cross-sections (free form surfaces). Compared with planar slices, curved cross-sections may easily follow the trajectory of tubular structures and organs such as the aorta or the colon. They may be extracted from a 3D volume, displayed as a 3D view and possibly flattened. Flattening of curved cross-sections allows to inspect spatially complex relationship between anatomic structures and their neighbourhood. They also allow to carry out measurements along a specific orientation. For the purpose of facilitating the interactive specification of free form surfaces, users may navigate in real time within the body and select the slices on which the surface control points will be positioned. Immediate feedback is provided by displaying boundary curves as cylindrical markers within a 3D view composed of anatomic organs, planar slices and possibly free form surface sections. Extraction of curved surface sections is an additional service that is available online as a Java applet (<http://visiblehuman.epfl.ch>). It may be used as an advanced tool for exploring and teaching anatomy.

CR Categories and Subject Descriptors: I.3.3 [Computer Graphics]: Picture/Image Generation - Viewing Algorithms; I.3.6 [Computer Graphics]: Methodology and Techniques - Interaction Techniques; J.3 [Computer Applications]: Life and Medical sciences.

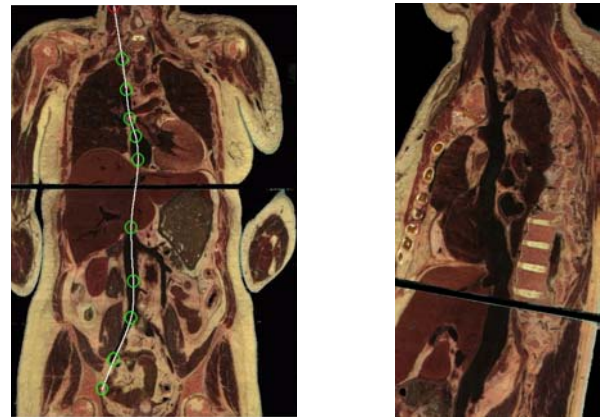
Additional Keywords: visualization, anatomic structures, curved sections, surface extraction, interactive flattening.

1 Introduction

State of the art tomographic imaging systems allow to visualize planar slices having an arbitrary orientation. Planar slices enable radiologists to inspect organs for diagnostic purposes. Planar slices are also useful for teaching anatomy. However, oblique planar slices do not always allow to adequately follow curved

anatomic structures. For instance, planar cross sections do not allow to see the continuity of tubular structures, such as the vena cava (Fig. 1a).

For visualizing such structures, one may specify and extract a ruled surface (Fig. 1b) from the original volume (an operation called curved planar reformation). However, ruled surfaces are not well suited for visualizing structures with many branches such as an arterial tree. Ruled surfaces are also too restricted for tracking anatomic structures with irregular geometry such as the pelvis. In this paper, we propose to extend the notion of cross section, which generally designates the extraction of a planar slice, to the extraction of free form surfaces. In contrast to planar slices, surfaces may follow curved anatomic structures. By flattening such surfaces, one may inspect these structures and their neighbourhood.



a) Planar slice

b) Flattened ruled surface

Figure 1. A ruled surface extracted from the Visible Human shows the continuity of the vena cava.

One challenge resides in offering interaction means facilitating the specification of surfaces following winded tubular structures within a 3D volume. To meet this challenge, we introduce surface specification tools which rely on interactive slicing and on the placement of marker points inside the volume. A second challenge resides in proposing a free form surface flattening paradigm meeting the expectation of the user, i.e. minimizing the distortions close to a curve of interest and preserving distances along a user specified orientation.

In Section 2, we outline possible approaches for surface extraction. In Section 3, we describe how to specify ruled surfaces along trajectories following tubular anatomic structures. In Section 4, we introduce our free form surface extraction and flattening methods. In Sections 5 and 6, we describe an application integrating interactive surface specification, extraction

*Peripheral System Laboratory,
{laurent.saroul, sebastian.gerlach, rd.hersch}@epfl.ch

and display, together with the display of the surrounding anatomic structures. Conclusions and possible future improvements are presented in Section 7.

2 Possible approaches

The simplest approach for specifying a ruled surface is to let the user specify a trajectory on an oblique slice and define the ruling vector perpendicular to this slice [Figueiredo and Hersch 2002]. For angiography applications, paths inside vascular tree structures may be computed and corresponding ruled surfaces may be extracted [He et al. 2001; Kanitsar et al. 2002]. These multiple surfaces are flattened onto the same image but discontinuities are unavoidable.

In order to be able to visualize branching structures without introducing discontinuities, we propose to lay out a Coons surface across the different branches of a tubular structure. Since the 3D display of a surface does not allow to inspect all surface parts within a single view, we introduce a user-driven flattening method particularly well suited for interactive applications.

Haker et al. [1999] propose a technique to flatten the brain surface both for anatomical study and for analyzing functional magnetic resonance images. A discretized Laplace Beltrami operator maps a topological sphere onto a disc by globally minimizing distortions. Similar methods are applied to the 3D visualization of colon CT images [Haker et al. 2000]. For cylindrical anatomic structures, attempts were made, for instance for virtual colonoscopy, to project the colon's surface onto a cylinder for virtual colonoscopy [Bartroli et al. 2001]. These surface flattening methods are not adapted to our problem since they are designed for the flattening of precomputed organ surfaces models and not for inspecting surfaces crossing sets of organs or tubular structures. Furthermore, they do not provide support for interactivity.

3 Specification and extraction of ruled surfaces

We first consider ruled surfaces for tracking curved anatomic structures. We focus our attention on ruled surfaces with a directrix $\alpha(t)$ and a ruling vector of constant orientation \vec{p} :

$$\sigma(t, \nu) = \alpha(t) + \nu \vec{p} \quad (1)$$

Such ruled surfaces are developable and easy to define, since they only require the definition of the directrix $\alpha(t)$ and of the ruling vector \vec{p} . A ruled surface may therefore be easily specified by a 2D natural spline located in a planar cross-section, with its ruling vector orthogonal to that cross section (Fig. 1).

However, a ruled surface whose directrix is located within a plane does not allow to easily visualize non-planar tubular structures such as the aorta. To provide support for specifying true 3D trajectories, we propose, by interactive slicing, to interactively move forward and backward within the 3D volume and place directrix control points (marker points) within the considered tubular structure, e.g. the aorta or the vena cava.

As ruling vector, we choose a vector orthogonal to the main orientations of the curve. Indeed, if the ruling vector is not adequately chosen, two ruling lines $\sigma(t_1, \nu)$ and $\sigma(t_2, \nu)$ may become identical, i.e. $\sigma(t_1, \nu) \equiv \sigma(t_2, \nu)$. Structures intersected by these lines may then be present at two different locations within the resulting flattened surface, making the image interpretation difficult. Compared with Kanitsar et al. [2002] where the ruling

vector has a fixed orientation within the (Oxy) plane, our method allows to compute the most adequate ruling vector automatically by avoiding as much as possible cases where ruling lines become identical. To offer additional freedom and improve the visualization, users are allowed to rotate the ruling vector in the plane orthogonal to the main orientation of the 3D trajectory.

The main orientations of the 3D trajectory are computed using principal component analysis. The trajectory is first represented by a polyline, i.e. a set of discretization points $S = \{\mathbf{x}_1, \mathbf{x}_2, \dots, \mathbf{x}_n\}$.

We compute the center of gravity G of this set, and the covariance matrix B , taking into account G and all points of S :

$$B = \frac{1}{n-1} \sum_{i=1}^n (\mathbf{x}_i - \mathbf{x}_G) (\mathbf{x}_i - \mathbf{x}_G)^T \quad (2)$$

Since covariance matrix B is symmetric, the normalized eigenvectors of B form a local coordinate system $(G, \vec{x}_a, \vec{x}_b, \vec{x}_c)$ with center G and axes $\vec{x}_a, \vec{x}_b, \vec{x}_c$. Vector \vec{x}_c is the vector orthogonal to the plane of principal components $(G, \vec{x}_a, \vec{x}_b)$ and is used as the ruling vector \vec{p} (Fig. 2).

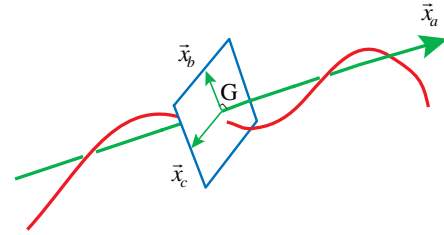


Figure 2. Computation of the ruling vector $\vec{p} = \vec{x}_c$.

We may change the orientation of the ruled surface by rotating ruling vector \vec{p} in the plane $(G, \vec{x}_b, \vec{x}_c)$

$$\vec{p}_\theta = \cos \theta \cdot \vec{x}_b + \sin \theta \cdot \vec{x}_c \quad (3)$$

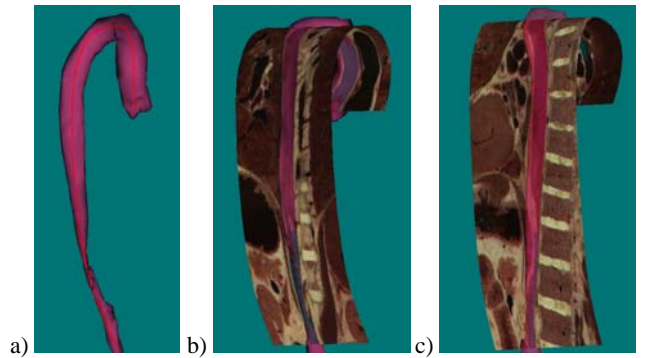


Figure 3. Extraction of ruled surfaces following the aorta, with different ruling vectors.

After discretization of the surface into rectangular facets, the labeled texture of the surface is extracted from the 3D volume image and visualized (Fig. 3). Such a ruled surface allows to visualize an entire section of the aorta together with its neighbourhood. By rotating \vec{p}_θ up to 180° , one may scan the full 3D neighbourhood of the considered trajectory.

In order to obtain a global view of the surface within a single image, one may flatten the ruled surface without introducing

angular or metrics distortions. The directrix $\alpha(t)$ is first approximated by a polyline, whose segments, together with the ruling vector, define a succession of rectangular facets. These rectangular facets are resampled according to the display grid. Corresponding voxels are extracted from the 3D volume data using nearest-neighbour or trilinear interpolation. Facets parts are then merged into the final display buffer (Fig. 4).

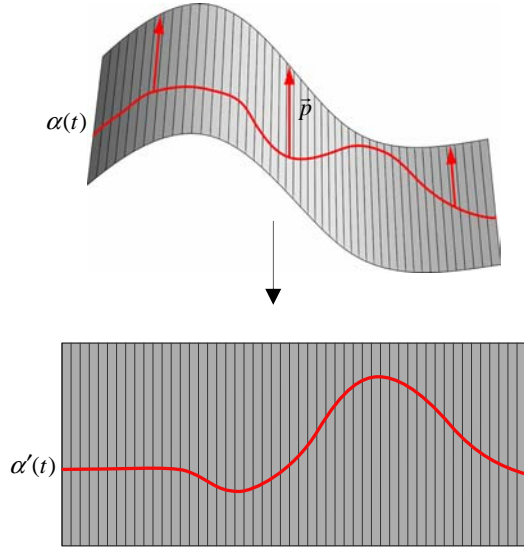


Figure 4. Flattening a ruled surface.

By being able to display the entire surface within a single image, one may quickly and precisely inspect it without having to rotate the view and possibly miss certain parts of the surface (Fig. 5).

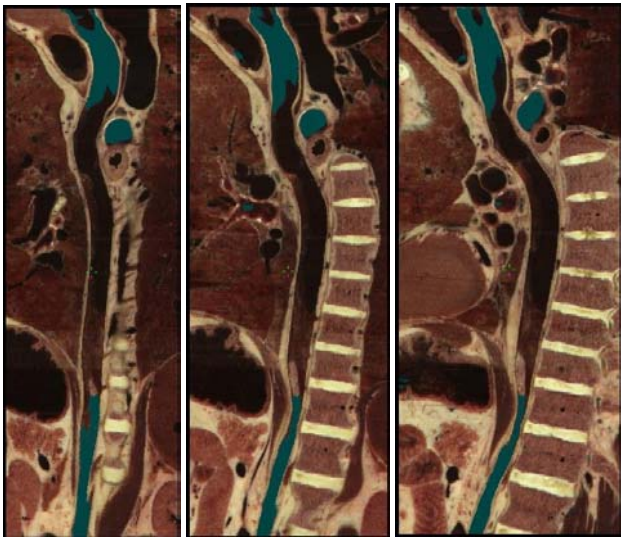


Figure 5. Flattened ruled surfaces following the aorta (with three different ruling vectors).

Since flattened ruled surfaces preserve distances, accurate distance measurements are possible. Furthermore, since each pixel on the flattened surface can be selected precisely, marker points can easily be placed and their 3D coordinates displayed.

4 Free Form Surfaces

Despite their usefulness, ruled surfaces do not offer enough flexibility for visualizing irregular anatomic structures such as the pelvis or the jaw. Furthermore, with a ruled surface, it is difficult to define a surface section that passes through a part of the aorta tree, i.e. the aorta together with its outgoing tubular structures. To offer a higher degree of freedom, we propose to use free form surfaces as visualization means.

The first difficulty is to find a method which enables an easy and accurate placement of a surface within a 3D volume. A second challenge resides in proposing an intuitive user-driven flattening method for free form surfaces.

Specification and extraction of free form surfaces

With Coons free form surfaces [Hoschek and Lasser 1993], users may interactively place boundary curves along structures of interest. The surface interpolates these boundary curves.

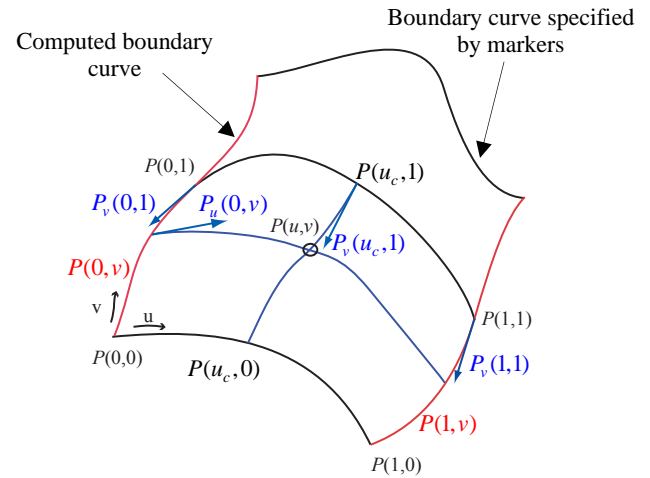


Figure 6. Surface interpolation between curves.

To facilitate the placement of the marker points defining the desired Coons surface boundary curves, users may navigate in real time across the volume (Section 5). On the desired slices, they may position marker points. Each set of successive marker points defines a surface boundary curve. The surface interpolating the boundary curves may then be extracted from the 3D volume and displayed in 3D, together with other related anatomic structures.

Let us describe the construction of Coons surfaces. Given n boundary cubic splines specified by the user, varying along the u parameter, the two other boundary cubic splines are constructed which pass through the extremities of these n curves (Fig. 6, red curves). The resulting system of boundary curves is interpolated by Coons patches [Hoschek and Lasser 1993, pp. 371-382]. Starting with the n curves specified by user, we can construct $n-1$ Coons patches by carrying out for each patch the following interpolation

$$P(u,v) = \left(P(u,0), P(u,1) \right) \begin{matrix} \textcircled{P} f_0(v) \\ \textcircled{P} f_1(v) \end{matrix} + \left(P(0,v), P(1,v) \right) \begin{matrix} \textcircled{P} f_0(u) \\ \textcircled{P} f_1(u) \end{matrix} - \left(f_0(u), f_1(u) \right) \begin{matrix} \textcircled{P} P(0,0) & P(0,1) \\ \textcircled{P} P(1,0) & P(1,1) \end{matrix} \begin{matrix} \textcircled{P} f_0(v) \\ \textcircled{P} f_1(v) \end{matrix} \quad (4)$$

where $P(i,v)$ and $P(u,i)$ are the parametric representations of the boundary curves for $i=0,1$ and where f_i are blending functions.

Since each boundary curve is a cubic spline with C^2 continuity, the corresponding patch has also C^2 continuity. We choose cubic Hermite polynomials as blending functions, which satisfy the continuity conditions

$$f_i(k) = \delta_{ik} = \begin{cases} 1, & i=k \\ 0, & i \neq k \end{cases} \quad \text{and} \quad f_i'(k) = 0, \quad \text{for } i,k=0,1. \quad (5)$$

Thus, derivatives of the patch along boundaries are given by

$$\begin{aligned} P_u(i,v) &= P_u(i,0) \cdot f_0(v) + P_u(i,1) \cdot f_1(v) \\ P_v(u,i) &= P_v(0,i) \cdot f_0(u) + P_v(1,i) \cdot f_1(u) \end{aligned} \quad \text{for } i=0,1. \quad (6)$$

Using these functions, the tangent vectors to the curve $P(u_c,v)$ at the point $P(u_c,1)$ (with u_c constant) depend only on the tangent vectors $P_v(0,1)$ and $P_v(1,1)$ at points $P(0,1)$ and $P(1,1)$. It follows from (6) that if the two computed boundary curves have C^1 continuity at these points, the two neighbouring patches A and B join together with C^1 continuity along the curve $P^A(u,1) = P^B(u,0)$ (Fig. 6). In contrast to bi-cubic patches [Hoschek and Lasser 1993, pp. 382-385], the presented bilinear interpolation with Hermite polynomials does not require to specify the derivatives along boundary curves $P_v(u,0)$, $P_v(u,1)$, $P_u(0,v)$ and $P_u(1,v)$.

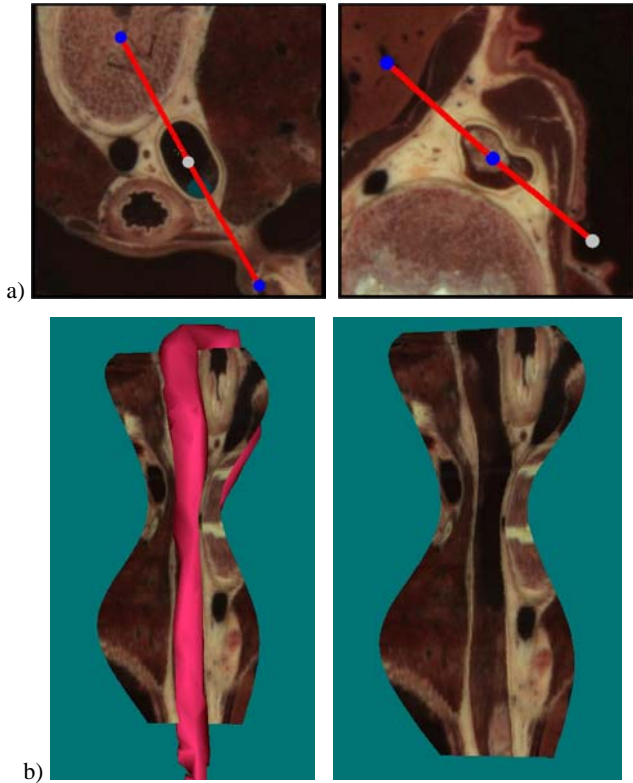


Figure 7. Curved section revealing the variation of the aorta lumen diameter.

As an example, a surface across the aorta is constructed by specifying boundary curves within several distant axial slices crossing the aorta (Fig. 7a). The boundary curves are oriented according to the lumen's main diameter. The resulting surface follows the largest aorta diameter and reveals diameter variations (Fig. 7b).

As a further example, we construct a surface passing through the aorta, the subclavian, the carotid and the brachiocephalic arteries. This surface is then extracted and displayed together with a 3D view of the aorta and the corresponding arteries (Fig. 8b) or alone (Fig. 8c). This allows to illustrate the connections between the aorta and the outgoing arteries.

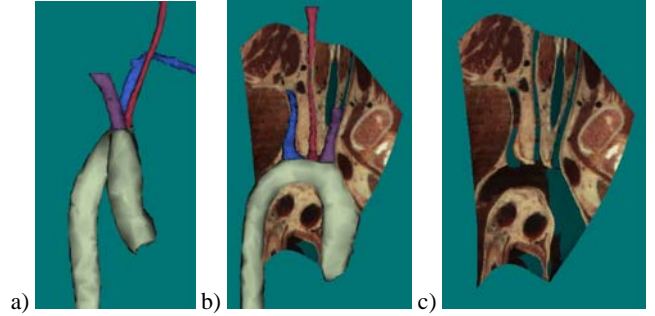


Figure 8. Curved section passing through a part of the aorta tree.

Flattening of Coons surfaces

Coons surfaces are not developable, i.e. it is not possible to unfold them without distortions. The unfolding of non developable surfaces is the inverse problem of texture mapping. In texture mapping, a planar image is mapped to a surface by globally minimizing distortions on the resulting 3D surface [Salomon 1999]. In our case, we would like to map a texture laid out on a surface onto the plane. Instead of globally minimizing distortions, we prefer to minimize distortions in a region of interest in order to inspect it with a higher precision. In addition, we may preserve distances along a user specified orientation. The user may then interactively modify the region of interest and the orientation of distance preservation in order to observe successive regions of interest.

In a previous approach to surface flattening, Bennis et al. [1991] unfold a parametric surface by flattening neighbouring transversal isoparametric curves C_v ($v=const$) so as to preserve both arc length and geodesic curvature (Fig. 9). This surface flattening method is not well suited for our application, since it does not provide an intuitive feeling about how metric distortions are distributed on the resulting flattened image. Indeed, within the flattened image, distances are not preserved along a specific direction but along curved lines (Fig. 9b, red curves).

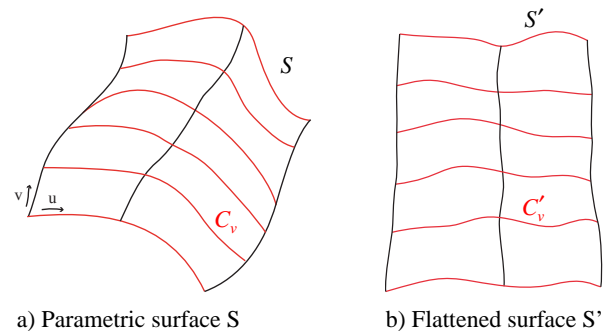


Figure 9. Flattening of a parametric surface according to Bennis et al. [1991].

Due to the preservation of the geodesic curvature along the curves, this method may also introduce self intersections between unfolded transversal curves. To provide a more intuitive

distribution of metrics distortions and allow to choose the desired orientation of distance preservation, we propose to reparameterize the surface before carrying out the flattening step. Such a reparameterization may ensure that transversal isoparametric curves correspond to the intersection between the surface and parallel planes of constant orientation. These transversal curves are then flattened into straight lines with distance preservation. In contrast to [Bennis et al. 1991], where arc length is preserved along curves defined by the initial parameterization, our method allows to choose the desired orientation of arc length preservation. In addition, by construction, it prevents the apparition of self intersections.

Algorithm Description

In a first step, the user selects a curve $C_{u_0} \{u = u_0, 0 \leq v \leq v_{\max}\}$ on the surface S as the reference curve for flattening purpose. The angular distortions will be minimized along this curve (Fig. 10). Then, a plane orientation $P = \{\vec{a}, \vec{b}\}$ is chosen according to the desired orientation along which distances should be preserved. One may define the plane orientation interactively or it may be computed automatically, e.g. as a plane orthogonal to the main orientation of the reference curve C_{u_0} .

By discretizing the surface along u , we obtain a set of curves C_u ($u = \text{const}$). For each sample point M_j of the initial curve C_{u_0} , the plane P_j of orientation P passing trough M_j is computed. The intersection points between P_j and the family of curves C_u provide a discrete representation of the intersection of the surface and plane P_j (Fig. 10)¹. By iterating along all sample points of C_{u_0} , we obtain a family of discrete curves C_h . Each discrete curve C_h corresponds to the intersection of a plane P_j and the family of curves C_u .

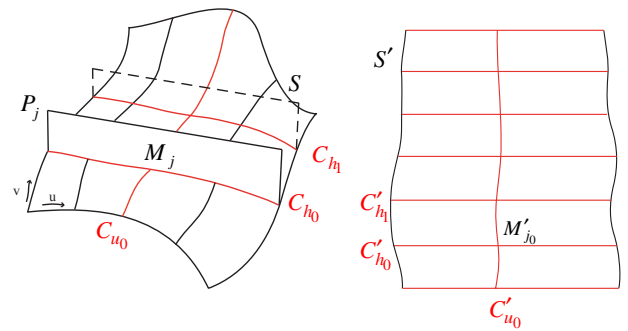
With the new parameterization defined by the family of curves C_u and the family of curves C_h , the flattening algorithm runs as follow:

1. Map the initial curve C_{u_0} into a plane by preserving the geodesic curvature² at each sample point and by preserving the distance between points, according to [Bennis et al. 1991] (see Appendix),
2. Map a curve C_{h_0} into a straight line with cross angle preservation between C_{h_0} and C_{u_0} and distance preservation between consecutive sample points of C_{h_0} ,
3. Map each curve C_h into a straight line parallel to C_{h_0} and passing through M'_j , with distance preservation between consecutive sample points of C_h .

By construction, this method preserves both the distances on the reference curve C'_{u_0} , and on the transversal curves C'_h . The cross angle between C_{u_0} and C_{h_0} is also preserved. The geodesic curvature is preserved along the reference curve C'_{u_0} , therefore angular distortions are minimized along a band of interest near the curve C'_{u_0} .

¹ In cases of double intersections between the plane P_j and the surface S , we choose the intersection curve closest to the previously computed intersection curve C_{h-1} .

² The geodesic curvature k_g of a curve $C(s)$ belonging to a surface S , at a point X , is the norm of the derivative of the tangential vector \mathbf{t}_g of $C(s)$ at X according to the arc length parameter s , i.e. $k_g = \|\mathbf{t}'_g(s)\|$.



a) Coons surface S b) Flattened surface S'

Figure 10. Flattening of a Coons surface preserving distances along a user-specified orientation.

Each facet (quadrilateral) of the resulting flattened surface is sampled according to the display grid. The corresponding colors are then extracted from the 3D volume image by nearest neighbour or trilinear interpolation.

Figure 11 shows a curved surface following the aorta and the corresponding flattened surface obtained with the algorithm described above. A grid showing the curves along which distances are preserved may be superposed on the flattened image (Fig. 11c). Since distances, within the resulting flattened image, are preserved along a constant orientation (Fig. 11c), the distribution of metric distortions becomes rather intuitive. Measurements may be carried out along that orientation.

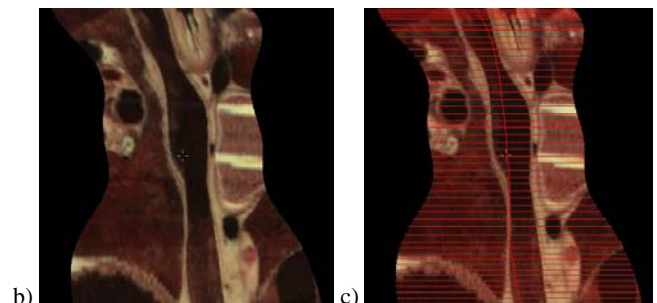


Figure 11. Flattening of a free form surface following the aorta.

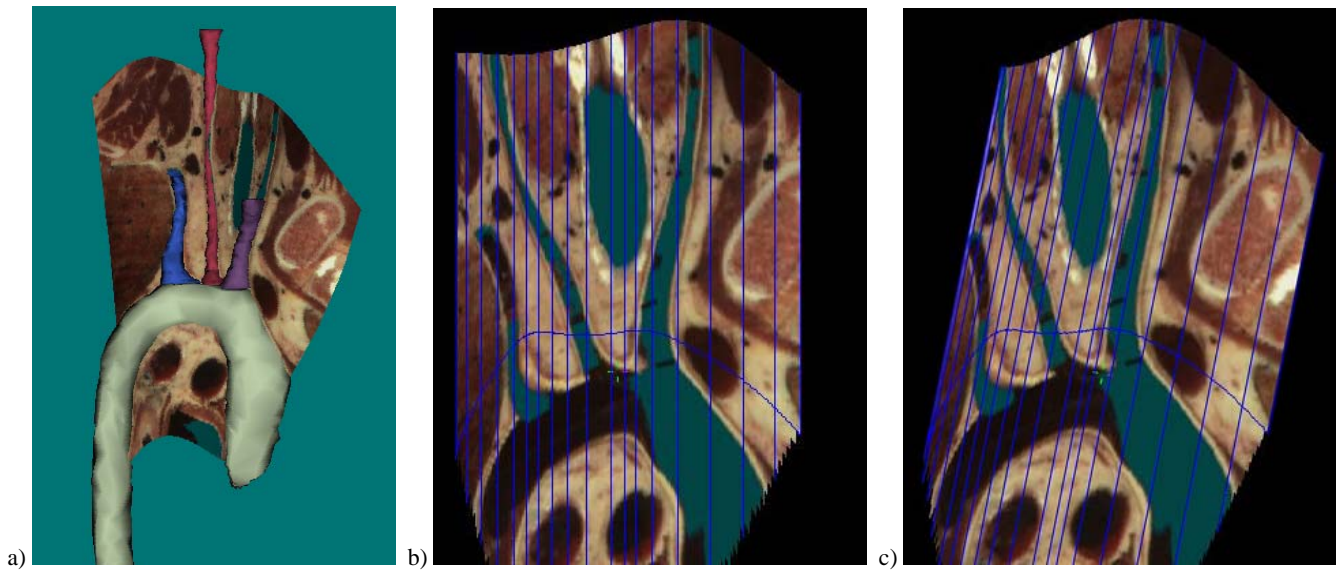


Figure 12. Flattening of a free form surface passing through the aorta tree with different orientations of distance preservation.

Figure 12 shows the flattening of a surface passing through the aorta tree. In order to minimize the distortions within a different area, one may choose another band of interest by selecting a different curve of reference. A different orientation of the planes P_j may also be specified (Fig. 12b and 12c). The new flattened surface is then recomputed.

The proposed surface flattening method provides a global view of a curved section within a single image, without introducing discontinuities. Distortions are present but the user may interactively choose their distribution and therefore inspect accurately all the surface parts. Flattened views may be used for illustrating properties of curved anatomic structures or for carrying out measurements along a user specified orientation.

5 Interactive specification of surfaces

In order to interactively specify in 3D space the boundary curves or trajectories defining a surface of interest, we use both interactive slicing across the volume image and the 3D display of organ surfaces and slices. Interactive slicing [Gerlach and Hersch 2002] enables navigating within the Visible Human volume image [Ackerman 1998] by continuously extracting slices at a speed of several slices per second, according to the displacement of the mouse (backward and forward translation, rotation, zoom). The 3D visualization interface [Evesque et al. 2002] allows users to construct 3D anatomical scenes by combining planar slices and 3D anatomical structures which may be selected and automatically loaded from the Visible Human server. User may zoom in and out, rotate and translate the scene as well as displace and rotate the planar slices located within the scene.

To accurately place points within the 3D volume, one should preferably use the interactive real time navigator for slicing through the volume data and halt on the slices on which marker points are to be specified. For understanding the 3D context, the current slice is displayed both in the real time navigator and in the 3D visualization interface, together with surrounding organ surface models (Fig. 13). At any time, both views may be

synchronized. This facilitates interactive and dynamic positioning of slices by mouse displacements.

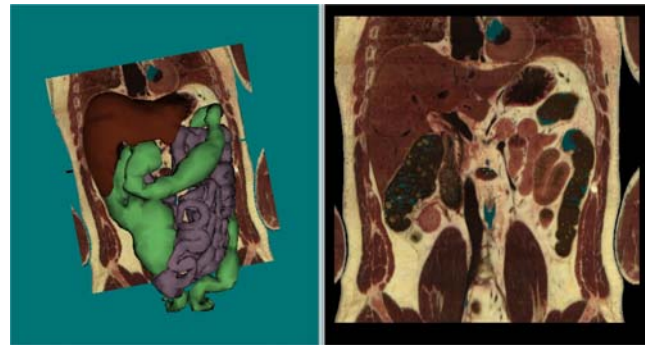


Figure 13. Synchronization between views.

Users may also modify the position of the slice in the 3D view by dragging it to the desired location and simultaneously see the corresponding movement in the slice navigator.

The presented approach relying on the synchronization between the slice navigator interface and the 3D viewer is similar to the approach of [Gering et al. 1999], used in surgical planning applications.

Interactive specification of trajectories and boundary curves

By combining the real time slice navigation and the 3D visualization interface, users may specify trajectories or boundary curves within the 3D volume by using markers. Markers are fat 3D cubic spline curves defined by several user-specified control points (marker points). Marker points may be freely placed by clicking with the mouse at the desired position on the selected slice. The markers are extruded as cylinders. Their intersection with the current slice is displayed (Fig. 14, right view).

However, the real time navigator does not provide a global view of the curve. The 3D visualization interface displays the marker as a 3D cylinder along the curve (Fig. 14, left view). By making organ models appear as partly transparent surfaces, the 3D curvilinear marker and its surrounding anatomic structures can be displayed simultaneously. In the example of Fig. 14, the aorta curve is displayed in transparency and reveals the 3D marker curve located inside it. Since both views are synchronized, the current marker shape is displayed in 3D while it is being specified by placing control points with the real time slice navigator. This ensures an optimal interactivity and an accurate placement of the marker splines.

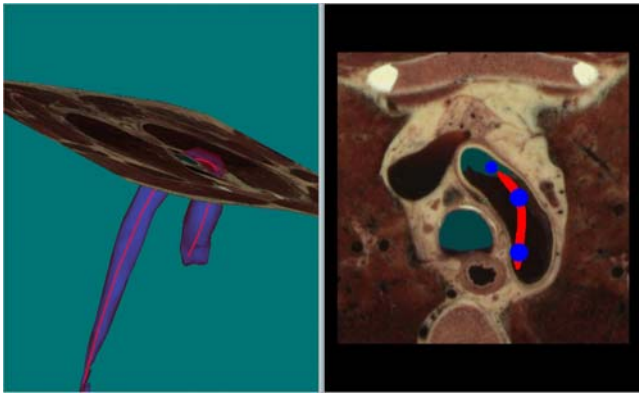
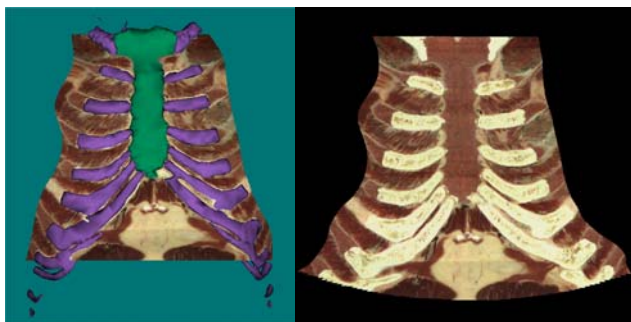


Figure 14. Simultaneous display of a marker in the slice navigator and in the 3D visualization interface.

6 Exploration of anatomic structures with surfaces and 3D models

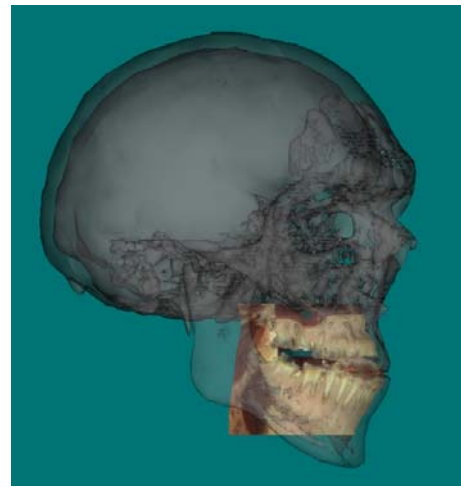
Let us summarize how users may make use of our interactive application to inspect anatomic structure of interest. In a first step, organ models surrounding the structures of interest are loaded and displayed in the 3D visualization interface (Fig. 15a). Then, using interactive slicing and thanks to the synchronized 3D display of the scene, marker points are positioned within the volume image. After specifying several boundary curves (markers), the application computes the resulting free form surface and requests from the server to extract the corresponding surface texture elements from the volume image. The surface elements are extracted from the 3D volume and sent back to the client for display. The boundary curves may be modified in order to adjust the shape or the location of the surface.



a) 3D view

b) Flattened view

Figure 15. Surface following the costal cartilage and the sternum.



a) 3D view



b) Flattened view

Figure 16. Surface section passing through the jaw.

Compared with conventional curved sections, free form surfaces allow to follow non tubular structures, such as the sternum and the costal cartilage. Figure 15 shows a surface passing through the sternum and costal cartilages and the resulting flattened image. Figure 16 shows a surface following the jaw. The flattened image reveals all teeth within a single image. The simultaneous display of surfaces and organs greatly facilitates the understanding and the interpretation of the flattened images.

Conclusions

In the present contribution, we generalize the concept of planar slices, which are widely used in medical imaging, to curved cross-sections. Curved cross-sections such as ruled surfaces or free form surfaces extracted from 3D volume images enable an accurate visualization of curved anatomic structures.

We integrate the curved cross-section extraction into an interactive slicing application allowing to visualize both the current slice and its representation within the surrounding anatomic scene. Combining the 2D slice view and the 3D scene view enables users to accurately position in 3D the control points determining the location and properties of the desired curved section. Free form surface boundaries as well as ruled surface trajectories are displayed as fat 3D cylindrical curves, visible both at their intersection with the current slice and within the 3D view.

Flattening of ruled and free form surfaces enables to follow curved anatomic structures. Free form surfaces are especially well

suited for tracking tubular tree structures such as the vascular or arterial trees. While the flattening of a ruled surface is straightforward, flattening of a free form surface needs to be intuitive, i.e. the user should be able to specify the regions of the surface which should be reproduced at a high fidelity. We present a first solution to the “interactive flattening” problem by minimizing distortions along a band of interest, i.e. a band whose central curve is a user-selected constant parameter curve. We also allow users to specify an orientation, along which distances are preserved.

For a thorough inspection of a surface, the user may successively select different bands of interest. He may also carry out measurements along the orientation along which distances are preserved. In the near future, we intend to further extend the interactive flattening paradigm in order to allow users to freely specify their region of interest and to provide information about the locations and the amplitudes of the distortions.

The present application is available on the Web, as an additional service offered by the Visible Human server (<http://visiblehuman.epfl.ch>). It provides both to the general public and to the professionals interested in anatomy an additional tool for visualizing complex anatomic structures and their intricate relationships.

Acknowledgements

The authors would like to thank Peter Ratiu from Harvard Medical School for creating the images of Figure 1. We also thank Jean Pierre Hornung, Beat Riederer and their students from the Medical School of the University of Lausanne for helpful discussions about the visualization interface and for suggesting anatomic structures of interest.

References

- ACKERMAN, M. 1998. The Visible Human Project, *Proc. of the IEEE*, Vol. 86, No 3, 504-511.
- BARTROLI, A.V., WEGENKITTL R., KÖNIG, A., AND GRÖLLER E. 2001. Virtual Colon Flattening, *Proc. of IEEE TCVG Symposium on Visualization*, 127-136.
- BENNIS, C., VÉZIEN, J.M. AND IGLÉSIAS, G. 1991. Piecewise Surface Flattening For Non-distorted Texture Mapping, *Computer Graphics, SIGGRAPH '91*, Vol. 25, No 4, 237-246.
- EVESQUE, F., GERLACH, S. AND HERSCH, R.D. 2002. Building 3D Anatomical Scenes on the Web, *Journal of Visualization and Computer Animation*, Vol. 13, 43-52.
- FIGUEIREDO, O. AND HERSCH, R.D. 2002. Parallel Unfolding and Visualization of Curved Surfaces Extracted From Large Three Dimensional Volumes, *Journal of Electronic Imaging*, Vol. 11, No 4, 423-433.
- GERING, D., NABAVI, A., KIKINIS, R., GRIMSON, W., HATA, N., EVERETT, P., JOLESZ, F., WELLS, F. 1999. An Integrated Visualization System for Surgical Planning and Guidance using Image Fusion and Interventional Imaging, *Proceedings of the Second International Conference on Medical Image Computing and Computer-Assisted Intervention (MICCAI)*, Springer Verlag, 809-819.
- GERLACH, S. AND HERSCH, R.D. 2002. A Real-Time Navigator For The Visible Human, *IEEE Internet Computing*, Vol. 6, No 2, 27-33.

HAKER, S., ANGENENT, S., TANNENBAUN, A. AND KIKINIS, R. 1999. On the Laplace-Beltrami Operator and Brain Surface Flattening, *IEEE Transactions on Medical Imaging*, Vol. 18, 700-711.

HAKER, S., ANGENENT, S., TANNENBAUN, A. AND KIKINIS, R. 2000. Nondistorting Flattening For Virtual Colonoscopy, *Third International Conference On Medical Robotics, Imaging and Computer Assisted Surgery*, Pittsburgh, Pennsylvania, USA.

HE, S., DAI, R., LU, B., CAO, C., BAI, H. AND JING, B. 2001. Medial Axis Reformation: A New Visualization Method For CT Angiography, *Academic Radiology*, Vol. 8, 726-733.

HOSCHEK, J. AND LASSER, D. 1993. *Fundamentals of Computer Aided Geometric Design*, AK Peters, 371-387.

KANITSAR, A., FLEISCHMANN, D., WEGENKITTL, R., FELKEL, P. AND GRÖLLER, M.E. 2002. CPR - Curved Planar Reformation, *Proc. of IEEE Visualization 2002 (Vis02)*, IEEE Press, 37-44.

SALOMON, D. 1999. *Computer Graphics & Geometric Modeling*, Springer, 552-556.

Appendix: Curve flattening with arc length and geodesic curvature preservation (according to [Bennis et al. 1991])

Let us recall that surface curves are approximated by polylines. A curve C that is to be mapped onto the plane contains $n+1$ sample points M_i , $i=0..n$. Let us denote by n_i and T_{p_i} , respectively, the normal vector and the tangent plane to the surface at point M_i . The curve flattening algorithm is the following:

1. Map the first curve segment M_0M_1 onto a segment P_0P_1 in the plane (Oxy) such that $d(M_0M_1) = d(P_0P_1)$, where d designates the Euclidean distance function.
2. For each j , $2 \leq j \leq n$, P_j is iteratively computed in the plane as follows:

- a) Project M_j and M_{j-2} onto the plane tangent to the surface at M_{j-1} . This provides two points in $T_{p_{j-1}}$, called \tilde{M}_j and \tilde{M}_{j-2} given by the formulas:

$$\tilde{M}_j = M_j + ((M_{j-1} - M_j) \cdot n_{j-1})n_{j-1}$$

$$\tilde{M}_{j-2} = M_{j-2} + ((M_{j-1} - M_{j-2}) \cdot n_{j-1})n_{j-1}$$

- b) Use a dilatation in $T_{p_{j-1}}$, in order to transform \tilde{M}_j into a point M'_j such that $d(M_{j-1}, M_j) = d(M_{j-1}, M'_j)$.

$$M'_j = M_{j-1} + \frac{\|M_j - M_{j-1}\|}{\|\tilde{M}_j - M_{j-1}\|} (\tilde{M}_j - M_{j-1})$$

- c) As P_{j-2} and P_{j-1} are already computed, the desired point P_j is the point of (Oxy) that preserves simultaneously the angle θ_{j-1} between $\tilde{M}_{j-2}M_{j-1}$ and $M_{j-1}M'_j$, and the distance $d(M_{j-1}, M'_j)$.

This curve flattening algorithm preserves the geodesic curvature at each sample point and the arc length between sample points.